Journal of Archaeological Science: Reports 34 (2020) 102663

Contents lists available at ScienceDirect

Journal of Archaeological Science: Reports

journal homepage: www.elsevier.com/locate/jasrep

Structural vulnerability of ancient dry masonry towers under lateral loading

Funda Gençer[a,*], Mine Hamamcıoğlu-Turan[b,1], Engin Aktaş[c,2]

[a] Department of Architecture, Manisa Celal Bayar University, Manisa, Turkey
[b] Department of Architectural Restoration, Izmir Institute of Technology, İzmir, Turkey
[c] Department of Civil Engineering, Izmir Institute of Technology, İzmir, Turkey

ARTICLE INFO

Keywords:
Ancient towers
Failure mechanism
Resistance
Dry masonry
Conservation

ABSTRACT

Understanding how the original characteristics contribute to the structural behaviour of antique structures should be the initial stage of planning for conservation work. This study aims to identify the structural behaviour of dry masonry towers under lateral loadings, so that the decision-making process when determining their restoration can be adequately supported. Dry masonry towers in ancient Caria, Pamphylia, and Cilicia Regions are examined. Each of these three areas have very different seismic characteristics. A hypothetical testing process was designed by combining different characteristics from each of the towers. As a result, the characteristics affecting the structural resistance were determined as; the staggering ratio, the stone depth, the ratio between block length and height, the proportional relationship between height and length, the area, number and position of openings, and the distribution of header stones. These characteristics all interact together to determine the failure mechanism; so, understanding this interaction is critical when considering conservation.

1. Introduction

When planning for structural conservation work establishing the original building characteristics, developed in antiquity, and their impact on the structural behaviour is paramount. Today, the majority of the defence structures in both Anatolia and Greece are in ruins or have been significantly altered since their original construction. In Caria, Pamphylia, Lydia, and Ionia regions, there are still many Hellenistic towers which have either been designed together with the city walls or as independent structures. Those from the early Roman period are observed in the Cilicia region and south-eastern Anatolia as independent structures (McNicoll, 8-11, 1997; Akarca, 141-148, 1998).

Earthquakes are a significant threat to the integrity of dry masonry towers, when compared to other threats, due to their vulnerability to lateral loading. Therefore, when considering the vulnerability of dry masonry towers, the threat posed by earthquakes should be of uppermost importance. Dry masonry towers are particularly vulnerable to lateral loading due to their intrinsic characteristics; such as wall profile, arrangement of openings, proportional relationships, material use, and ground topography as well as the sub-categories of these characteristics such as the block staggering ratio, and the area, position and number of openings, etc.

The sub-categories of these characteristics have been tested through experimental (Jimenez, 2011; Restrepo Vélez et al., 2014), computational (Bui et al., 2017; Ferrante et al., 2020) and analytical methods (Vaculik et al., 2004; D'Ayala and Speranza, 2003) in preliminary studies seeking to establish the structural vulnerability of dry masonry walls. Most of the studies in literature examine only a one or two sub-categories by analyzing the in-plane or out-of-plane behaviour of a wall, or of a wall with one or two side walls (Giuffré, 1996; Vaculik et al., 2004; De Felice, 2011; Jimenez, 2011; Foti et al., 2018). There are very few studies examining more than two sub-categories. However, even in these studies the sub-categories are only examined in isolation without taking into account the interactions between them (Giuffre et al., 1994; Shi et al., 2008; Shi, 2016; Vaculik, 2012; Restrepo Vélez et al., 2014). In addition, the data used in these studies was based purely on fictional structures, rather than real dry masonry buildings.

There are a number of methods available for analysing the structural

* Corresponding author at: Faculty of Fine Arts, Design and Architecture, Department of Architecture, Manisa Celal Bayar University, Halil Erdoğan Street, District of Ahmet Bedevi, Şehzadeler, Manisa 45040, Turkey.
E-mail address: funda.gencer@cbu.edu.tr (F. Gençer).
[1] Orcid id: 0000-0002-7418-9577.
[2] Orcid id: 0000-0002-5706-210.

https://doi.org/10.1016/j.jasrep.2020.102663
Received 13 February 2020; Received in revised form 12 October 2020; Accepted 1 November 2020
Available online 13 November 2020
2352-409X/

vulnerabilities of various construction configurations, taking into account a range of different characteristics, but the quasi-static analysis method was deemed to be the most suitable. The quasi-static analysis is based on equilibrium and strength methods (Jimenez, 2011; DeJong, 2009). Tilt analysis can be carried out by physical models in the laboratory environment (Giuffre et al., 1994; Vaculik et al., 2004; Shi et al., 2008; Jimenez, 2011; Restrepo Vélez et al., 2014), while 3D simulation models can be carried out using computers, with different approaches (Azevedo and Sincraian, 2000; De Felice, 2004; Da Costa, 2012). The computer analysis can then be validated using the experimental analysis results (Giuffre, Pagnoni, and Tocci, 1994; De Felice and Giannini, 2001; Vaculik, 2012; Bui et al., 2017; Foti et al., 2018). Although analysis using physical models in the laboratory environment is highly reliable, it is also highly time-consuming, often requiring a large budget, and requiring a considerable amount of man-hours. In contrast, 3D model simulations, validated by experimental methods, provide a quick and practical understanding of the lateral load resistance of dry masonry towers (Bui et al., 2017).

Within this setting, this study aims to identify the structural behaviour of dry masonry towers under lateral loading, considering their original characteristics, so that the decision-making process in relation to their restoration, can be properly supported. Emphasis is made on both the collapse angles and failure mechanisms of the towers. This enables a general understanding of the basic behaviour of these towers, under lateral loading. The relationship between the characteristics and the behaviour of six dry masonry towers, under lateral loading, in ancient Caria, Pamphylia, and Cilicia on the Aegean and Mediterranean coasts, are examined (Fig. 1). It is also worth noting that the ground accelerations vary significantly across these different regions (AFAD, 2018).

2. Methodology and tools

The following approach uses a combination of quasi-static analysis together with conventional methods of architectural conservation. The work is undertaken in three phases: documentation of the characteristics of the case study towers; impact analysis of hypothetical towers designed by a combination of the characteristic types, and an examination of the analysis results (Fig. 2).

The documentation phase considers a selection of case studies and determines the characteristics of each case. When selecting case studies, building type was established as a constant factor in the analysis. Dry masonry watch towers in three different earthquake regions; Caria (with an extremely high earthquake threat), Pamphylia (with a high earthquake threat), and Cilicia Regions (with a low earthquake threat) were chosen as the main focus to understand the effect of earthquake threat on characteristics of towers (AFAD, 2018). The impact on the structural strength from the following characteristics could be compared: masonry techniques, the relationship between height and length, the opening types, and the material types. The towers that were most complete and had not undergone current restoration work, were selected as case studies. There were six dry masonry ancient towers considered: Alinda and Latmos in Caria, Sillyon, and Perge in Pamphylia, Gömeç, and Sarayın in Cilicia. Their structural and morphological characteristics have been documented by traditional documentation techniques and their material usage is investigated using laboratory analysis.

The impact analysis phase consisted of determining and combining the characteristics of real towers, with the design, and tilt analysis of hypothetical towers, to determine their collapse angles and failure mechanisms. Hypothetical towers were designed based on a combination of different characteristics. These towers were modelled as individual rigid blocks positioned together without any connecting elements, in SketchUp 2017. MS Physics 1.0.3 software was then used for the quasi-static tilt analysis simulation, based on the equilibrium state. This allowed real-time physical simulation of discrete elements, where each element could be given specific properties such as shape, density, and friction, etc. It was a static rigid body approach to solve the equilibrium problem (Synytsia, 2018).

Preliminary analyses were carried out to test the validity of the MS Physics software. Simulation results were compared with the experimental results in the literature (Restrepo Vélez et al., 2014, 1–28).

Based on the wall sizes and properties of materials, produced by Restrepo-Vélez, Magenes, and Griffith (2014), 3D models were created using SketchUp software, and the failure mechanisms were investigated by tilting these models using a virtual table in MsPhysics. Restrepo Vélez et al. (2014) performed a comprehensive quasi-static testing programme, considering 1:5 scale models of dry-joint stone masonry walls and buildings, using marble units. The dimensions of their marble blocks were 80 mm × 40 mm × 30 mm. The friction of blocks was taken as 0.77 and their unit weight was 2680 kg/m^3 (Bui et al., 2017). (Kinetic friction was calibrated at 0.67). A typical specimen in this quasi-static testing programme had a height of 0.6 m, equivalent to 21 courses. The specimens were one, two- or three-sided walls, with or without openings, with different staggering ratios, and also included a two-story building with openings similar to the tower walls.

To ensure accuracy in the 3D model computer simulations, an update time step of 1/120 was taken and the iterative value of 16 was chosen. The damage mechanisms and collapse angles of the real verses the virtual models were found to be almost identical (Table 1, Fig. 3).

Thus, the MsPhysics software was deemed to be sufficient to gain an understanding of the effect that structural characteristics had on the collapse angle and failure mechanism. MS Physics software provides rigid block, group, and component densities based on the connection states and physical simulations. In the simulations, the friction coefficient is taken into consideration, but the modulus of elasticity is ignored. This is based on studies in literature (D'Ayala and Speranza, 2003). The update time step was taken as 1/120 since a smaller update time step provides more accurate simulation results and prevents collisions from deteriorating. Since the towers were composed of many moving blocks, the iterative value was taken as 16 (Synytsia, 2018). The floor and roof elements and the interaction between the tower and the city walls have not been taken into consideration, as the majority of these towers have very limited information for these characteristics. This study focused on those structures with authentic construction techniques and building geometry where their integrity has, in general, been preserved. Similarly, structural failures stemming from previous lateral loading, settlement, vandalism, weathering, etc. have not been included in the modelling process.

Altering the lateral acceleration applied to each 3D model was achieved by tilting the ground plane of the model. The value of tilt was increased by one degree until total collapse occurred. The component, parallel to the tilted ground plane of the gravitational acceleration at the level of collapse, may be interpreted as corresponding to the peak ground acceleration the structure is required to resist. The horizontal acceleration (λ) is equal to the lateral component of the gravitational acceleration, where: $\lambda = mg \times \sin\theta$ (DeJong, 2009; Jimenez, 2011). While this equivalent static loading does not represent the effects of dynamics, as presented through seismic loading, it makes it possible to measure the lateral load-bearing capacity of the structure in terms of acceleration. Each designed tower was tilted in two directions taking into consideration variations in the positioning of openings: openings within both in-plane and out-of-plane walls. The smallest collapse angle was always considered for the evaluation. In-plane and out-of-plane behaviour of the walls was evaluated based on definitions developed by Giuffrè (1993), and D'Ayala and Speranza (2003). Total tower failure mechanisms were identified with the help of the studies of Bazan and Meli (2003), and Milani et al. (2018). All failure mechanisms were described in sequence of their events. Additional definitions were proposed, if necessary.

Collapse angles and failure mechanisms of each hypothetical tower were determined with the results gained through the tilt analysis. Effective characteristics were filtered based on the results. Then, sub-

Fig. 1. Towers in Caria, Pamphylia and Cilicia.

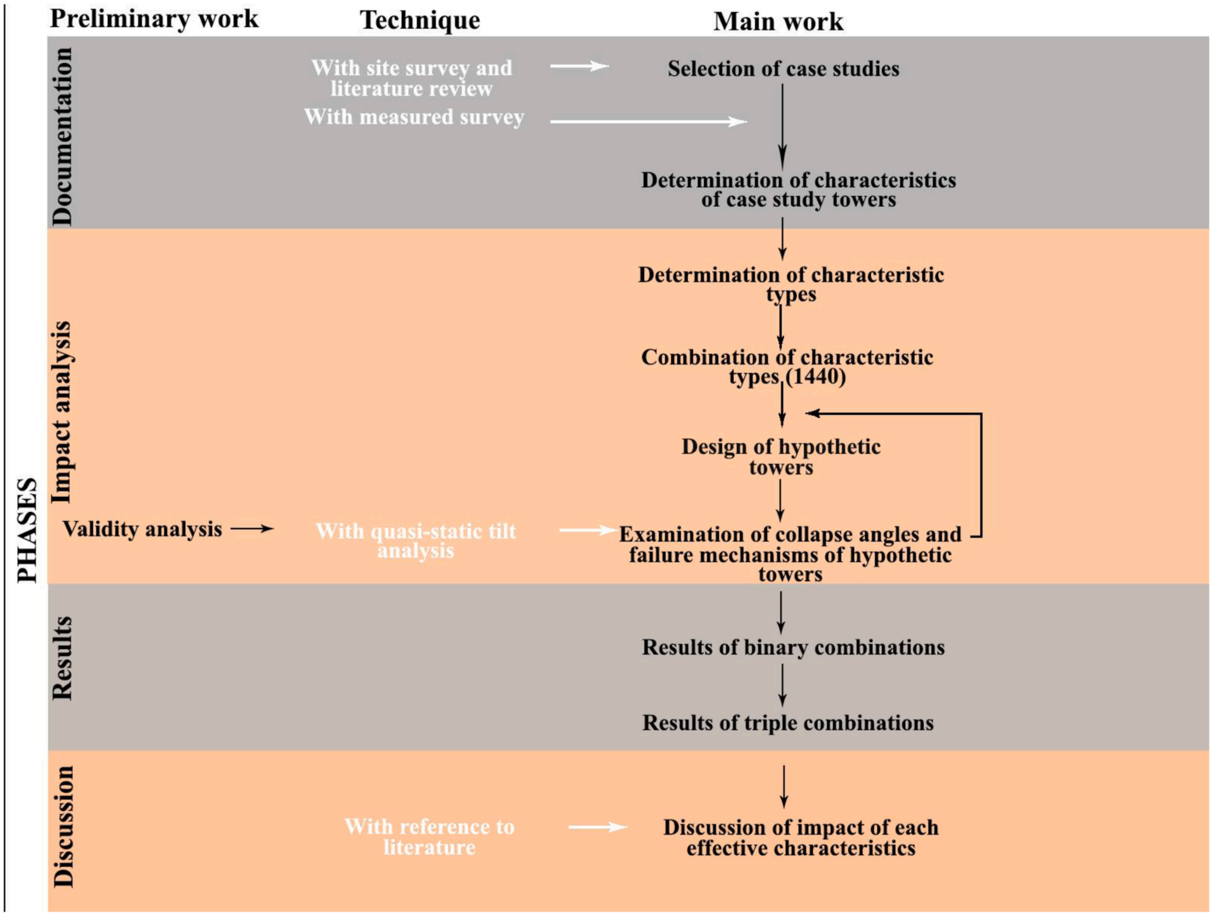

Fig. 2. The methodology of the study.

categories that shape each effective characteristic were discussed with respect to the literature review.

3. Impact analysis of characteristics

The impact analysis phase was composed of both the design and analysis of the hypothetical towers. In the design phase the structural, morphological and material characteristics of the towers were identified, based on data gathered through documentation. Possible characteristic types were then combined.

The towers were selected in three different earthquake regions: Caria, Pamphylia, and Cilicia Regions. The towers have different properties in different regions, so parameters were determined depending on the regions. Blocks were laid using the header and stretcher technique, with two outer leaves and a gap, in the towers of Caria Region, alternating header and stretcher rows were used in the Pamphylia Regions, and the classical isodomic masonry-style was observed in the Cilicia Region. These wall profiles show differences in terms of the arrangement and size of blocks, the wall thicknesses and the number of leaves, either single or double-leaf, depending on region. Six wall profile types were determined (Fig. 4).

For the proportional relationships, data regarding wall thicknesses, length, and height values were examined. Studies in literature demonstrate that the ratio between height and length (slenderness) (h/l) is critical for the structural behaviour of towers (Shi et al., 2008; Romaro, 2011). The height of towers is mostly around 1000 cm, while the length is in the range of 475 and 775 cm. In the Cilicia Region, Gömeç Tower has narrow facades, therefore the h/l ratios are higher (around $h/l = 2.3$). In the Caria Region, due to the ground slope, the walls have differing h/l values. Latmos tower has smaller h/l values due to its short facade looking toward the mountain ($h/l = 1.6$). The h/l values of other towers vary between 1.8 and 2. Four different height to length ratios were therefore chosen (1.6, 1.8, 2, and 2.3) (Fig. 4).

Tower openings vary in their positions, size, and number. When all possibilities were combined, 15 opening types were determined. Whether an opening is positioned in the out-of-plane or the in-plane wall relative to the direction of the lateral loading, is important in determining the structural behaviour of the tower (Fig. 4).

Based on laboratory analysis, two main types of stone were established: granite and limestone. Granite was used in the towers of the Caria Region, while limestone was preferred in the Pamphylia and Cilicia Regions. These results are also supported by data regarding stone sources of the regions (McNicoll, 1997).

In the studies about the behaviour of dry masonry walls in literature, the coefficient of friction values are critical. Since the walls were constructed without mortar, the shear strength along the joints is provided purely by friction (Restrepo Vélez et al., 2014; Bui et al., 2017). The friction coefficient of rock blocks in masonry varies between 0.6 and 0.7 (Concrete Institute, 1909, 144). Established friction values for granite and limestone were accepted (limestone: 0.72; granite: 0.6) (Concrete Institute, 144, 1909; Colas et al., 2016; Jay, 224, 1908).

The density value is critical for dynamic analysis, therefore different density values have not been tested. The modulus of elasticity of the materials is neglected because the displacements due to elastic deformation are negligible.

Two ground topography conditions were chosen: positioning on flat and inclined topography.

The six wall profiles, the four ratios between wall height and length, the 15 openings, the two material types, and the two ground topographies were then combined, giving 1440 hypothetical towers. These

Table 1
Comparison of results of experimental analysis and simulations.

Configurations Restrepo Vélez et al. (2014)	Results of experimental analysis Restrepo Vélez et al. (2014)		Results of simulation		Individual errors of lateral accelerations
	Collapse angle	Lateral acceleration	Collapse angle	Lateral acceleration	
S1-2–3 (two sided wall, F = 11 bricks, S = 4 bricks)	15	0.254 g	16	0.275 g	−0.083
S4 (two sided wall, F = 11 bricks, S = 4 bricks, 3 mm vertical joint gaps)	9	0.161 g	8	0.14 g	0.130
S5 (two sided wall, F = 8 bricks)	20	0.349 g	19	0.325 g	0.069
S6 (two sided wall, F = 13 bricks, S = 4 bricks)	12	0.208 g	12	0.208 g	0.000
S7 (two sided wall, F = 8 bricks, S = 7 bricks)	17	0.291 g	18	0.309 g	−0.062
S8 (two sided wall, F = 6 bricks, S = 7 bricks)	21	0.362 g	20	0.343 g	0.052
S10 (one sided wall, F = 12 bricks, S = 10 bricks)	12	0.213 g	13	0.22 g	−0.033
S11 (one sided wall, F = 12 bricks, S = 10 bricks)	5.5	0.097 g	6	0.104 g	−0.072
S12 (one sided wall, F = 8 bricks, S = 7 bricks)	7	0.129 g	7	0.121 g	0.062
S13 (one sided wall, F = 6 bricks, S = 7 bricks)	10	0.181 g	9	0.15 g	0.171
S14 (t-wall, F = 6 bricks, S = 7 bricks)	14.5	0.251 g	14	0.24 g	0.044
S15 (t-wall, F = 8 bricks, S = 7 bricks)	11.5	0.199 g	11	0.19 g	0.045
S16 (t-wall, F = 12 bricks, S = 10 bricks)	8	0.139 g	7	0.12 g	0.137
S17 (t-wall, F = 6 bricks, S = 7 bricks)	12	0.207 g	14	0.24 g	−0.159
S18 (t-wall, F = 8 bricks, S = 7 bricks)	13.3	0.230 g	12	0.207 g	0.100
S19 (t-wall, F = 12 bricks, S = 10 bricks)	9	0.151 g	9	0.156 g	−0.033
S20 (three sided wall, F = 14 bricks, , S = 10 bricks)	16.5	0.285 g	17	0.292 g	−0.025
S21 (three sided wall, F = 14 bricks, S = 10 bricks)	14.2	0.244 g	16	0.275 g	−0.127
S22 (three sided wall, opening at the side walls, F = 14 bricks, S = 10 bricks)	11.4	0.197 g	12	0.207 g	−0.051
S23 (two sided wall, two openings on the front wall F = 14 bricks, S = 10 bricks)	8.5	0.144 g	9	0.15 g	−0.042
S24 (two sided wall, two openings at the front wall F = 14 bricks, S = 10 bricks)	9.1	0.156 g	11	0.19 g	−0.218
S30 (two sided wall, F = 8 bricks, S = 7 bricks, weak connection, s/h = 0.7 only at the corners)	14.8	0.255 g	17	0.292 g	−0.145
S31 (two sided wall, F = 8 bricks, S = 7 bricks, s/h = 0.7 along the side walls)	10.2	0.177 g	11	0.19 g	−0.073
S42 (two storey building with openings)	13.7	0.236 g	12	0.207 g	0.123

Average of absolute errors:-0.008.
F = length of the front wall S = side walls.

hypothetical towers were initially analysed, but it was discovered that the narrow proportional relationship range for height and lengths did not reveal any advantages or disadvantages. Therefore, the range of proportional ratios was expanded, whilst ensuring that the characteristics chosen were sensible. To determine the impact of h/l, towers with h/l ratios of 1.15, 1.3, and 2.5 were also added. Whilst some of these hypothetical towers had h/l ratios that exceeded those of the real towers, the actual height and length values were kept within the range of the real tower values ($915 \le h \le 1405$, $475 \le l \le 780$), (1.15 h/l = 915/780; 1.3 = 915/700; 6 = 960/600; 2 = 1200/600; 2.3 = 1380/600). Extra-long or high towers were not considered.

4. Results of analysis

The collapse angles of the hypothetical towers varied between 7 and 19 degrees. There were four types of failure mechanisms determined through this analysis: out-of-plane (mechanism A and G), in-plane (mechanism B1 and B2), hybrid (a combination of in-plane and out-of-plane mechanisms; mechanism B_2 + G), and total body failures (B_{2T}) (Table 2) (Giuffrè, 1993; D'Ayala and Speranza, 2003; Preciado et al., 2016; Milani et al., 2018). Total body failure can be combined with in-plane or out-of-plane wall failures (Mechanism B2T + DT).

The results demonstrated that wall profile type, positioning of openings, and the ratio between height and length impacted the failure mechanisms and the collapse angles of towers. However, the rock material or ground topography did not impact upon the collapse angle or failure mechanism. When the towers were tilted from the tallest wall façade towards the shortest one, the collapse angle increased by one degree in all wall profiles with all characteristic combinations. In the reverse direction, the collapse angle was equivalent to that of the tower being located on flat ground. However, wall profile 1 was not impacted by the increase of inclination. Ground topography did not change failure mechanisms.

The wall profile preferences altered the collapse angle by up to twelve degrees. The resistance to lateral loading of the different wall profile types is evaluated as wall profile types 6, 4, 5, 3, 2, and 1 from the most durable to the least durable. Opening types 1–9 and 12 and 13 did not impact on the collapse angles of the wall profile (Table 3). These opening types will be referred to as 'negligible impact openings' throughout the text. The behaviour of those towers where the openings had negligible impact demonstrated typical failure mechanisms based on wall profiles. Wall profile 6 resulted in total overturning (B_{2T}) (Table 4; purple letters). Wall profile 4 resulted in the collapse of the sidewalls, due to in-plane cracking (B_2). Wall profile 5 resulted in total overturning combined with vertical splitting (B_{2T+VS}). Wall profiles 1, 2, and 3 resulted in hybrid failure mechanisms; the collapse of the two side walls due to in-plane cracking followed by the out-of-plane overturning of the facade wall, due to vertical cracking at the corner connection (B_2 + A) (Table 4; pink letters). However, while in-plane cracking occurs relative to the upper openings in wall profiles 2 and 3, in-plane cracking occurs at the upper parts of the wall profile 1, prior to the out-of-plane overturning of the façade. The in-plane failure is not related to the openings in the wall profile 1 (Fig. 5; Table 4). This means that the wall profile characteristics of profile 1, that cause out-of-plane failure, are more dominant than openings.

Different opening types can alter the collapse angle by up to 4 degrees. The smallest collapse angles (indicated in bold black letters) are seen with openings 10, 11, 14, and 15 (Table 3). These opening types will be referred to as 'critical openings' throughout the text. 'Significant impact openings' mainly result in in-plane failure mechanisms. There is not necessarily a change in the typical failure mechanisms of wall profiles solely due to these openings. Mechanism B_2 is the most widespread

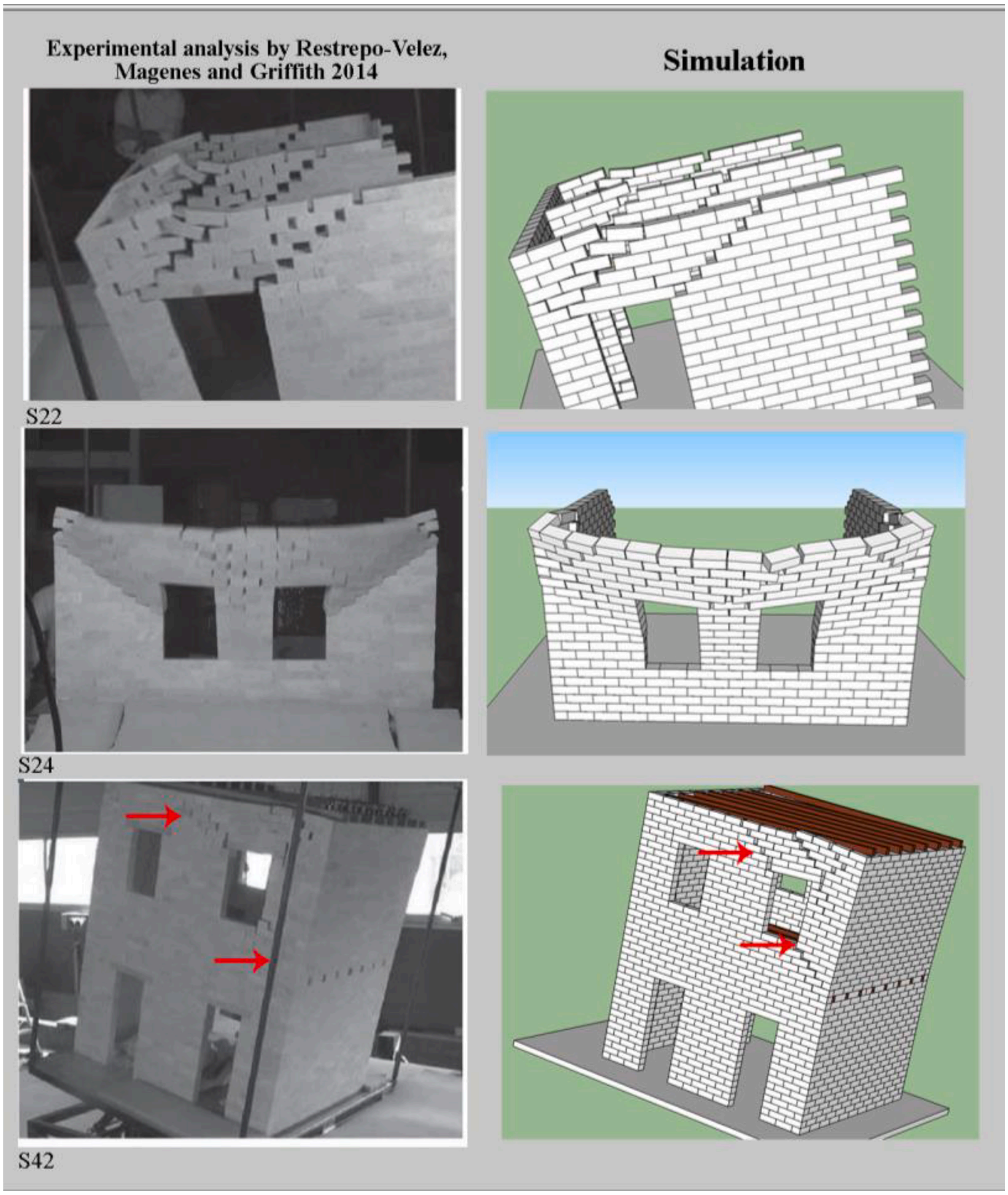

Fig. 3. Validation of the method (Restrepo Vélez et al., 2014).

failure observed in the smallest collapse angles of all of the wall profiles. Opening 10 causes mechanism B_2, the collapse of two side walls with in-plane diagonal cracks. The effect of opening 10 is seen most distinctly on wall profiles 5 and 6 (Fig. 6), since opening 10 causes mechanism B_2 in place of total overturning. Failure mechanism B_1 followed by B_2 is directly related to the opening being located in the in-plane position: it is mostly seen in openings 8, 11, 14, and 15 (Fig. 7; Table 4; bold letters).

When openings are in the out-of-plane position, the collapse angle is approximately up to 3 degrees higher than the collapse angle with openings in the in-plane position (Table 3). Openings in the out-of-plane position cause mechanism G; detachment of the façade wall due to diagonal cracks downwards from the corners in wall profiles 1, 2, and 3. While openings do not affect the failure mechanism of wall profile 4. The effects of openings in the out-of-plane position can be seen in wall profiles 5 and 6, which have typical total failure behaviour. Openings result in either mechanism G alone, in wall profile 5, or a combination of the detachment of the rear facade wall together with overturning due to bending in wall profile 6 (mechanism B_{2T+DT}) (Table 4).

The collapse angles for those towers with h/l ratios of between 1.6 and 2, are mostly constant and have the highest values. When the ratio decreases and increases beyond this range, the collapse angle decreases (Table 3). The towers sustain typical failure mechanisms for height to length ratios of between 1.6 and 2.3, which are realistic relationships (Fig. 8; Table 4; blue letters). The worst h/l ratios for wall profiles are ratios smaller than 1.3 and higher than 2.3 h/l ratios (the lowest 2 degrees of each wall is accepted as the worst).

Out-of-plane failures (mechanism A, G or DT) occur at ratios smaller than 1.3 when a 'negligible impact opening' is present. Mechanism G occurs at wall profile 1, mechanism A occurs at wall profiles 2 and 3. Mechanism A is combined with the typical failure mechanism for wall profile 4 (B_2 + A). Wall profile 5 demonstrates in-plane behaviour (B_2) in place of total body behaviour. In addition, even if the strongest wall profile, profile 6, sustains its total body behaviour, detachment of the rear facade is combined with mechanism B2T + DT, at h/l ratios smaller than 1.3 (Fig. 8; Table 4; blue letters).

h/l ratios smaller than 1.3 cause out-of-plane behaviour in cases with

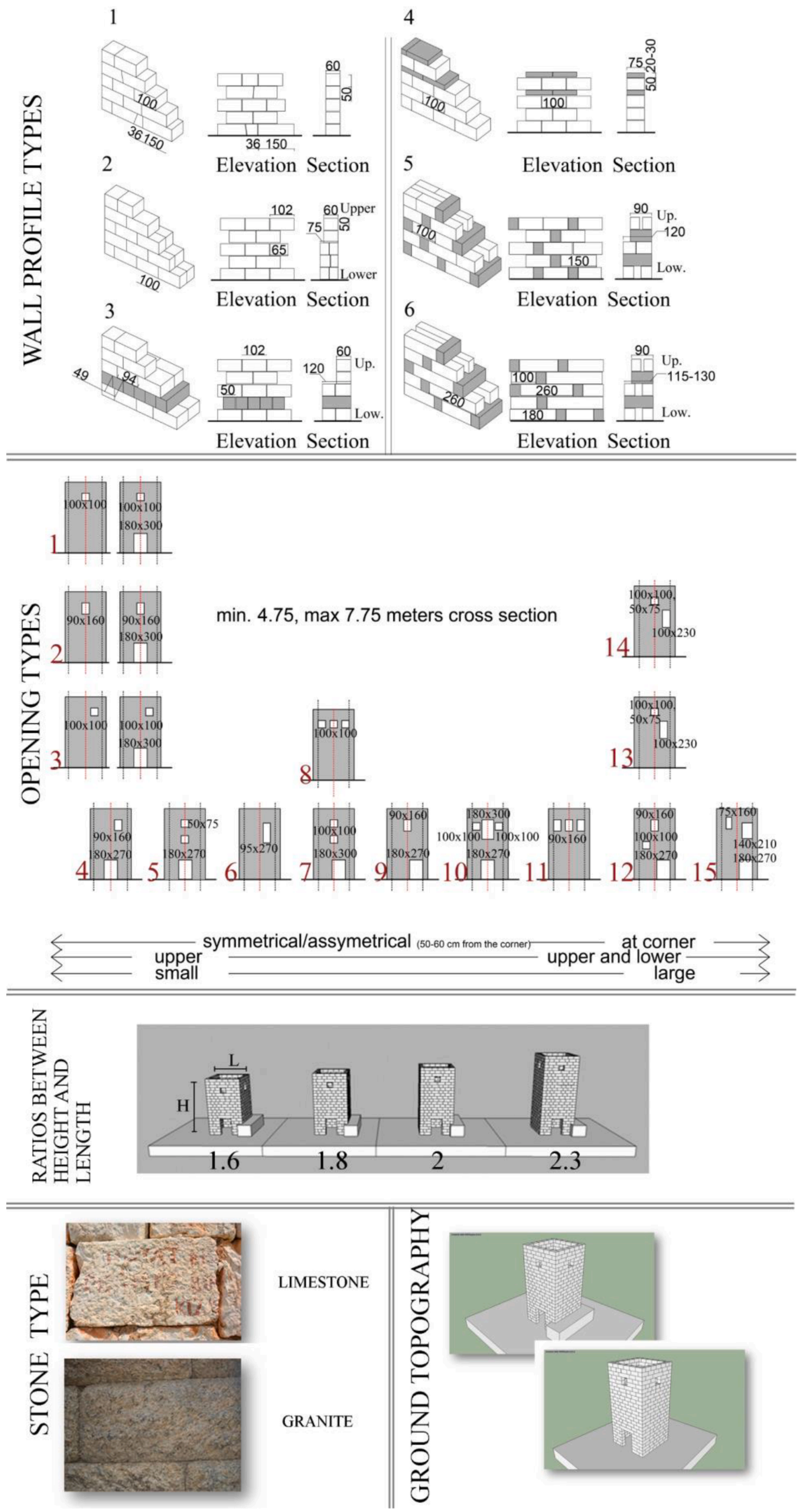

Fig. 4. Characteristic types.

Table 2
Determined failure mechanism types of masonry walls of towers (D'Ayala and Speranza, 2003; Giuffrè, 1993; Bazan and Meli, 2003; Preciado et al., 2016).

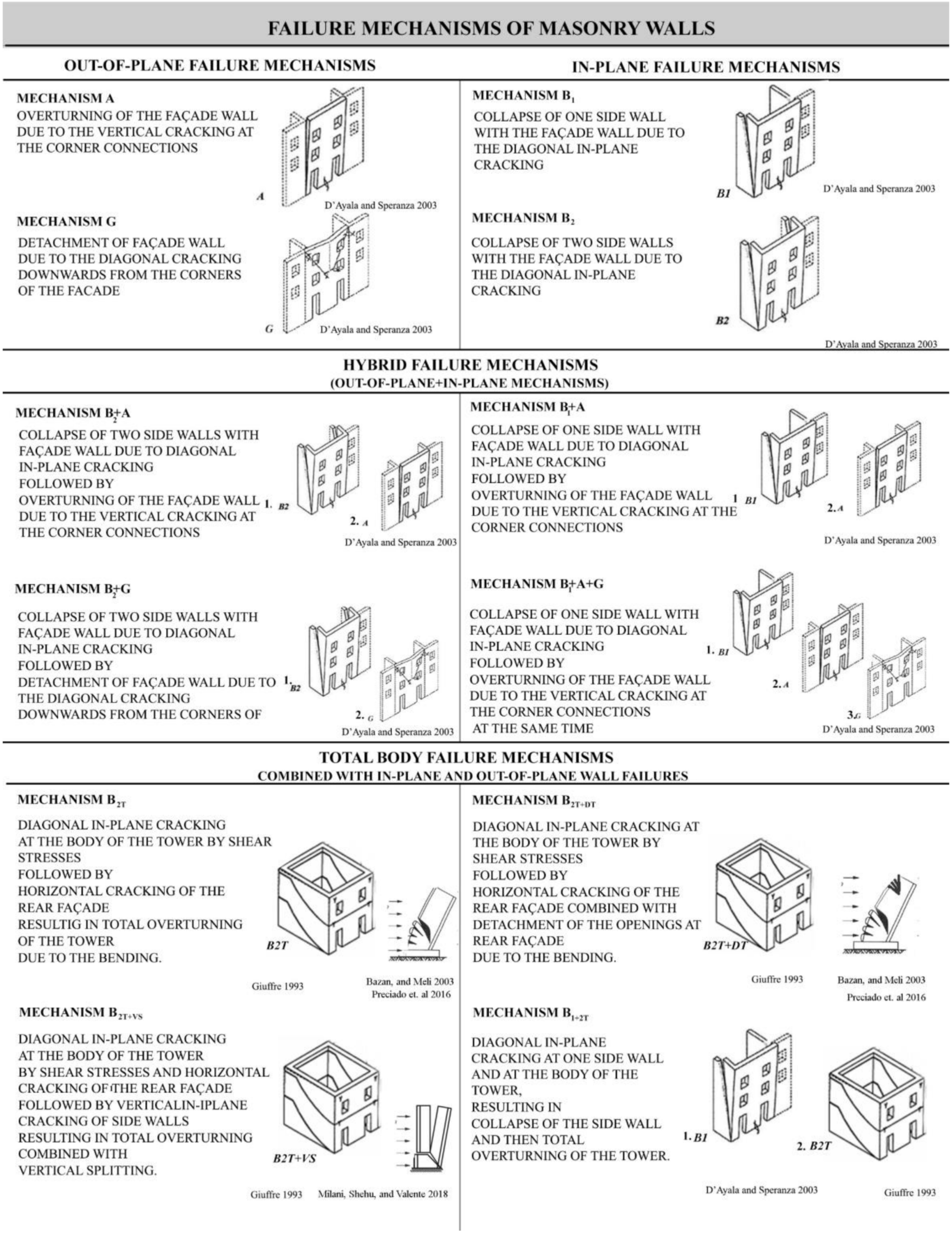

'negligible impact openings'. However 'significant impact openings' in the in-plane position are dominant for all ratios including those smaller than 1.3. Opening 10, which is the dominant opening type, causes mechanism B_2 for all wall profile types regardless of the h/l ratio, even if it is smaller than 1.3 (Table 4; Fig. 9). Openings 8, 11, 14, and 15 are also dominant. However, the out-of-plane mechanism, caused by ratios smaller than 1.3, can combine with the in-plane mechanism resulting from openings (Fig. 10). However, the out-of-plane behaviour as a result of small h/l ratios are not seen in wall profiles 4, 5, and 6 with openings 8, 11, 14, and 15 (Table 4).

Openings in the out-of-plane position result in mostly out-of-plane failures for all ratios. However, wall profile 4 (B_2) and 6 (B_{2T}) sustain their typical failure mechanisms at ratios higher than 1.6, regardless of the opening types, except for opening 10. Opening 10 is dominant in the out-of-plane position and causes detachment of the facade wall (mechanism DT of G) for all ratios and all wall profile types (Table 4).

Table 3
Collapse angle (°) results of a triple combination of effective characteristics.

		Height / Length													
		1		1.3		1.6		1.8		2		2.3		2.5	
	Opening types	i	o	i	o	i	o	i	o	i	o	i	o	i	o
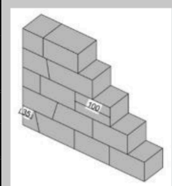 w. profile 1	op 1	7		8		11		11		11		11		10	
	op 2-8	7	7	8	8	11	11	11	11	11	11	11	11	10	11
	op 9, 12-13	7	7	8	8	10	11	10	11	10	11	10	11	9	10
	op 10	6	7	8	8	**9**	11	**9**	**10**	**8**	**9**	**8**	**10**	**8**	**10**
	op 11	7	7	8	8	**9**	11	**9**	11	**9**	11	**8**	**10**	**8**	11
	op 14, 15	7	7	8	8	**9**	11	**9**	11	**9**	11	**9**	**10**	**8**	**10**
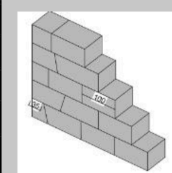 w. profile 2	op 1	9		11		12		12		12		12		12	
	op 2-8	9	9	11	11	12	12	12	12	12	12	12	12	12	12
	op 9	9	9	11	11	12	12	12	12	11	12	11	12	11	11
	op 10	9	9	**10**	11	**11**	12	**11**	12	**10**	12	**10**	12	**9**	**11**
	op 11	9	9	**10**	11	**11**	12	**11**	12	**10**	12	11	12	10	**12**
	op 12-13	9	9	11	11	12	12	12	12	11	12	**10**	12	**9**	11
	op 14, 15	9	9	11	11	**11**	12	**11**	12	**11**	12	**9**	**11**	**8**	**10**
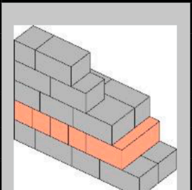 w.profile 3	op 1	11		13		14		14		13.5		13.5		13	
	op 2-8, 12-13	11	11	13	13	14	14	14	14	13.5	13.5	13.5	13.5	13	13
	op 9	11	11	13	13	14	14	14	14	13	13.5	13.5	13.5	13	13
	op 10	**10**	11	**12**	13	**12**	14	**12**	14	**12**	13.5	**12**	13.5	**11**	13
	op 11	**10**	11	**12**	13	**12**	14	**12**	14	**12**	13.5	**12**	13.5	**11**	13
	op 14, 15	**10**	11	**12**	13	**12**	14	**12**	14	**12**	13.5	**12**	13.5	**11**	13
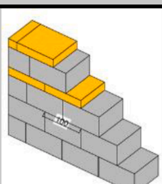 w. profile 4	op 1	14		16		17		17		17		16		15	
	op 2-9, 12-13	14	14	16	16	17	17	17	17	17	17	16	16	15	15
	op 10	**12**	14	**13**	16	**15**	17	**15**	17	**14**	17	**13**	**15**	**12**	**14**
	op 11	**13**	14	15	16	17	17	17	17	16	17	16	16	**13**	15
	op 14, 15	**13**	14	15	16	17	17	17	17	16	17	15	16	**13**	15
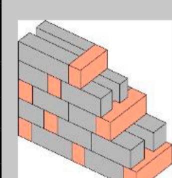 w. profile 5	op 1	12		13		15		15		14		14		13	
	op 2-5, 8, 12-13	12	12	13	13	15	15	15	15	14	14	14	14	13	13
	op 6, 9	11	12	12	13	14	15	14	15	13	14	13	14	12	13
	op 10	**10**	**11**	**11**	**12**	**12**	15	**12**	15	**12**	14	**12**	**13**	**11**	**12**
	op 11	**10**	**11**	**11**	**12**	13	15	13	15	13	14	**12**	14	12	13
	op 14, 15	**10**	**11**	**11**	**12**	13	15	13	15	13	14	**12**	14	12	13
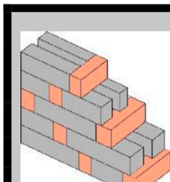 w. profile 6	op 1	17		19		19		19		18		16		15	
	op 2-9, 12-13	17	17	19	19	19	19	19	19	18	18	16	16	15	15
	op 10	**15**	**16**	**18**	19	**18**	19	**18**	19	**17**	18	16	16	15	15
	op 11	16	17	**18**	19	**18**	19	19	19	18	18	16	16	15	15
	op 14, 15	16	17	**18**	19	19	19	**18**	19	18	18	16	16	15	15

*__Hatch:__ best h/l performance intervals of each wall profile type, **Bold letter:** opening types causing the worst resistance for each wall profile type

Table 4
Failure mechanisms results of a triple combination of effective characteristics.

		Height/Length									
		1-1.3		1.6		1.8		2		2.3-2.5	
	Opening	i	o	i	o	i	o	i	o	i	o
w. profile 1	1	G		B_2+A		B_2+ A		B_2+A		B_2+A	
	2-7	G	G	B_2+A	G	B_2+A	G	B_2+ A	G^{ST}	B_2+A	G
	9, 12, 13	G	G	B_2+A	G	B_2+A	G	B_2+A	G^{ST}	B_2+A	G
	10	B_2	G	B_2	G	B_2	G	B_2	G^{ST}	B_2	G
	8, 11	B_1+A+G	G	B_1	G	B_1	G	B_1	G^{ST}	B_1	G
	14	B_2+A	G	B_2+A	G	B_2+A	G	B_2+ A	G	B_2+A	G
	15	B_1+A	G	B_1	G	B_1	G	B_1	G	B_1	G
w. profile 2	1	A		B_2+A		B_2+A		B_2+A		B_2+A	
	2-9	A	G	B_2+A	G	B_2+A	G	B_2+A	G	B_2+A	G
	3-7,12, 13	B_2+A	G	B_2	G	B_2	G	B_2	G	B_2+A	G
	10	B_2	G	B_2	G	B_2	G	B_2	G	B_2	G
	8, 11	B_2+A	G	B_2	G	B_2	G	B_2	G	B_2	G
	14	B_2+A	G	B_2	G	B_2	G	B_2	G	B_2	G
	15	B_1	G	B_2	G	B_2	G	B_2	G	B_2	G
w. profile 3	1	A		B_2+A		B_2+A		B_2+A		B_2+A	
	2-7	A	G	B_2+A	B_2+A	B_2+A	B_2+A	B_2+A	B_2+A	B_2+A	B_2+A
	9, 12, 13	A	G	B_2+A	B_2+G	B_2+A	B_2+A	B_2+A	B_2+A	B_2+A	B_2+A
	10	B_2	G	B_2	B_2+G	B_2	B_2+G	B_2	B_2+G	B_2+A	B_2+A
	8, 11	B_2+A	G	B2+A	G	B_2+A	G	B_2+A	G	B_2	G
	14	B_2+A	B_2+A	B2+A	B_2+A	B_2+A	B_2+A	B_2+A	B_2+A	B_2+A	B_2+A
	15	B_1	G	B_1	G	B_2	G	B_2	G	B_2	G
w. profile 4	1	B_2+A		B_2		B_2		B_2		B_2	
	2-8	B_2+A	B_2+A	B_2	B_2	B_2	B_2	B_2	B_2	B_2	B_2
	9, 12, 13	B_2+A	B_2+A	B_2	B_2	B_2	B_2	B_2	B_2	B_2	B_2
	10	B_2	B_2+G	B_2	B_2+G	B2	B_2+G	B_2	B_2+G	B_2	B_2+G
	8, 11	B_1	B_2	B_2	B_2	B_2	B_2	B_2	B_2	B_2	B_2
	14	B_2	B_2	B_2	B_2	B_2	B_2	B_2	B_2	B_2	B_2
	15	B_1	B_2	B_2	B_2	B_2	B_2	B_1	B_2	B_1	B_2
w. profile 5	1	B_2		B_2		B_{2T+VT}		B_{2T+VT}		B_{2T}	
	2, 5-7, 9, 12,13	B_2	G	B_{2T+VT}	B_{2T+DT}	B_{2T+VT}	B_{2T+DT}	B_{2T+VT}	B_{2T+DT}	B_{2T+VT}	B_{2T+DT}
	3,4	B_2	G	B_{2T+DT}	B_{2T+VT}	B_{2T+DT}	B_{2T+VT}	B_{2T+DT}	B_{2T+VT}	B_{2T+DT}	B_{2T+DT}
	10	B_2	G	B_2	B_2+G	B_2	B_2+G	B_2	B_{2T+DT}	B_2	B_{2T+DT}
	8, 11	B_1	G	B_1	G	B_1	G	B_1	B_{2T+DT}	B_1	B_{2T+DT}
	14	B_2	G	B_2	G	B_{2T+VT}	B_{2T+DT}	B_{2T+VT}	B_{2T+DT}	B_{2T+VT}	B_{2T+DT}
	15	B_1	G	B_1	G	B_1	G	B_1	B_{2T+DT}	B_1	B_{2T+DT}
w. profile 6	1	B_{2T+DT}		B_{2T}		B_{2T}		B_{2T}		B_{2T}	
	2-7, 9, 12	B_{2T+DT}	B_{2T+DT}	B_{2T}	B_{2T}	B_{2T}	B_{2T}	B_{2T}	B_{2T}	B_{2T}	B_{2T}
	13	B_{2T+DT}	B_{2T+DT}	B_{2T}	B_{2T+DT}	B_{2T}	B_{2T+DT}	B_{2T}	B_{2T}	B_{2T}	B_{2T}
	10	B_2	B_{2T+DT}	B_2	B_{2T+DT}	B_2	B_{2T+DT}	B_2	B_{2T+DT}	B_{2T}	B_{2T}
	8, 11	B_1	B_{2T+DT}	B_1	B_{2T+DT}	B_1	B_{2T+DT}	B_{2T}	B_{2T}	B_{2T}	B_{2T}
	14	B_2	B_{2T+DT}	B_2	B_{2T+DT}	B_{2T}	B_{2T}	B_{2T}	B_{2T}	B_{2T}	B_{2T}
	15	B_1	B_{2T+DT}	B_1	B_{2T+DT}	B_1	B_{2T+DT}	B_{2T}	B_{2T}	B_{2T}	B_{2T}

* Table 4 contains the legend of Table 3. **Letters** also represent the change of failures. **Purple:** total body behavior; **Pink:** out-of-plane behavior due to the wall profile types. **Blue:** out-of-plane behavior due to h/l ratios smaller than 1.3. **Bold:** change of failure with the effects of openings.

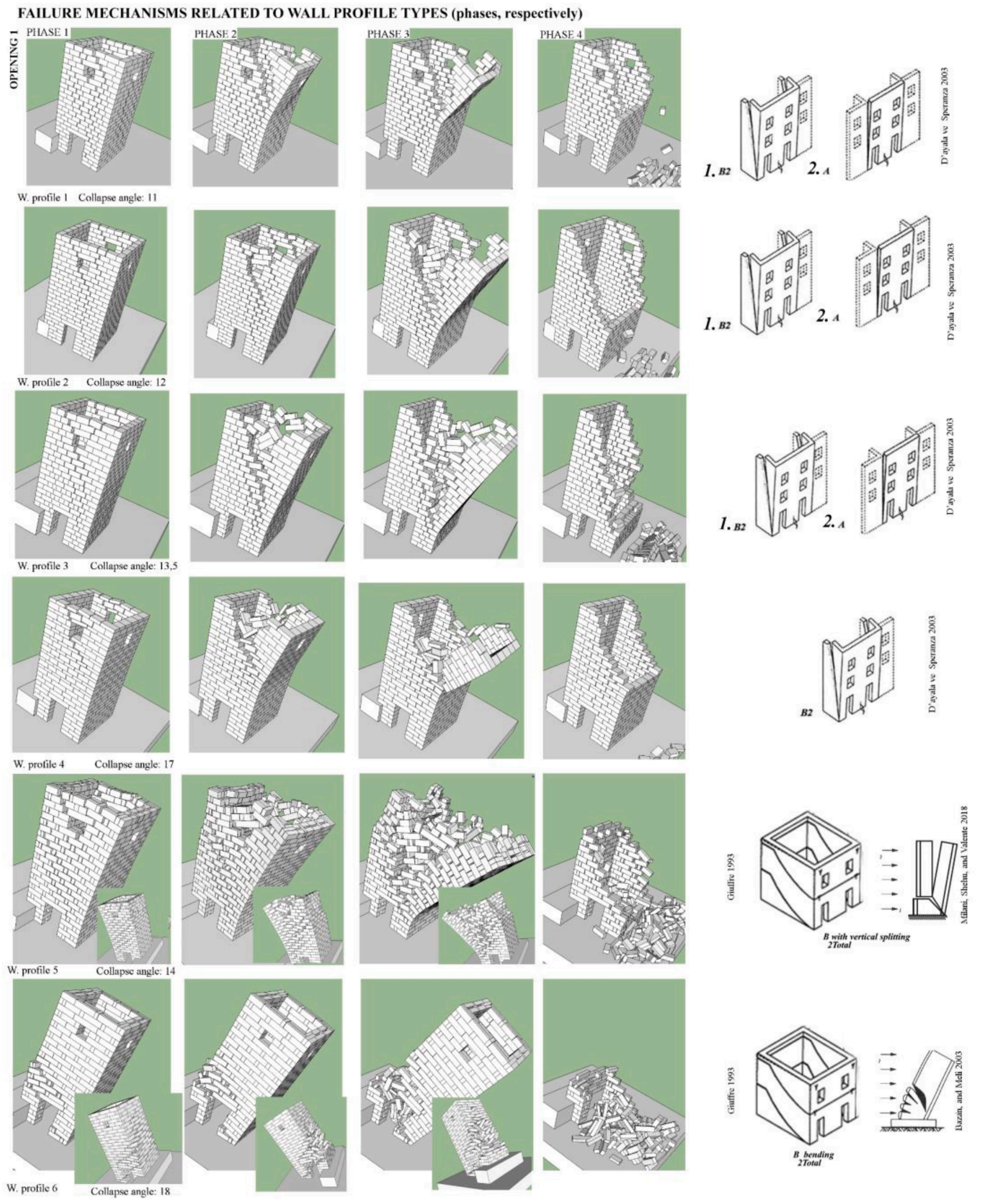

Fig. 5. Typical failure mechanisms and collapse angles of wall profile types (Giuffrè, 1993; D'Ayala and Speranza, 2003; Bazan and Meli, 2003; Milani et al., 2018).

5. Discussion

Variation in failure mechanisms and collapse angles are discussed depending on the sub-categories of the effective characteristic types, wall profiles, proportional relationships, and positioning of openings.

5.1. Wall profile

Staggering ratio, the ratio between block length and height, the number of leaves, the upper stone depth, and the usage of headers are all sub-categories related to the wall profile (Table 5).

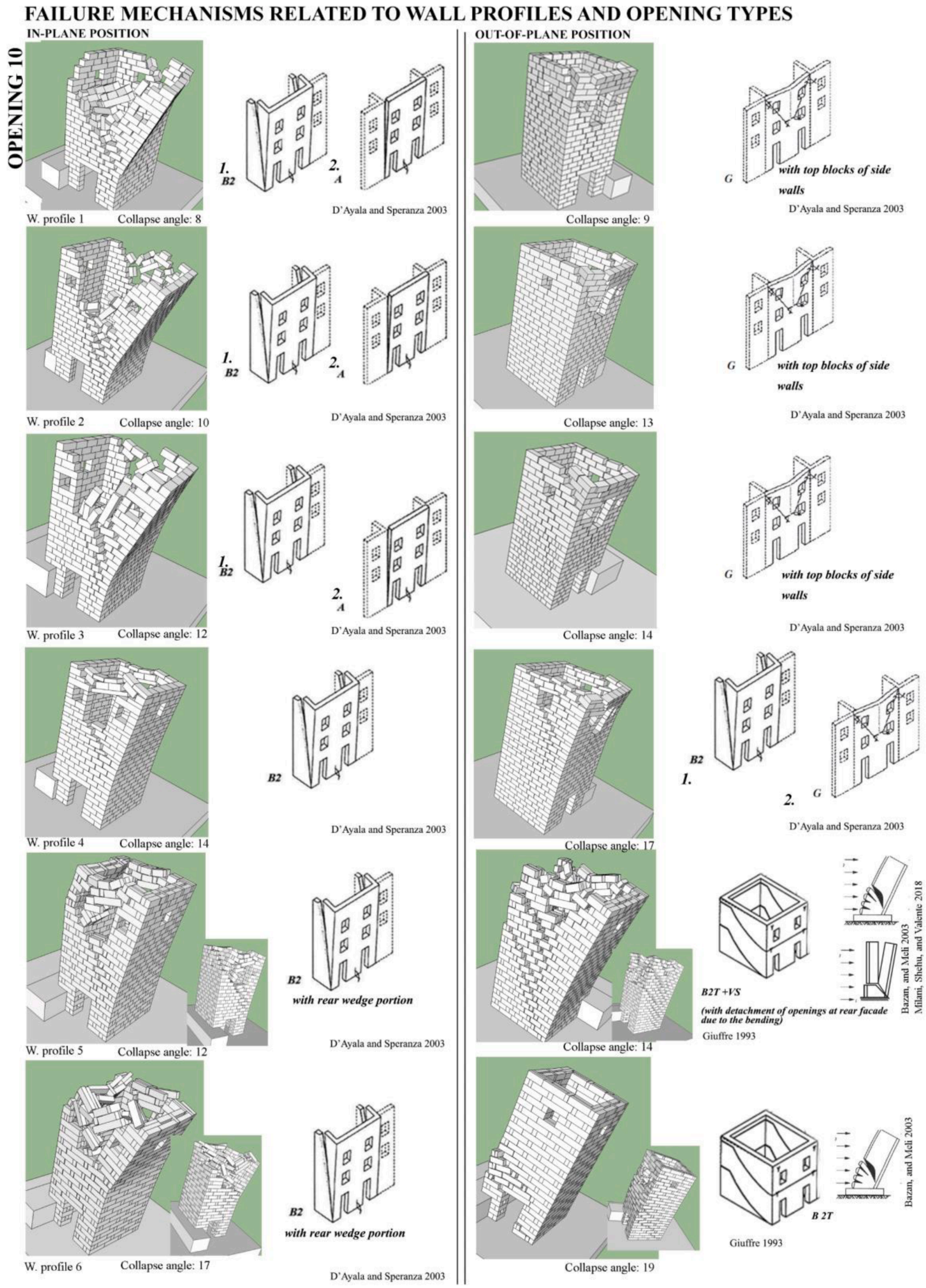

Fig. 6. Failure mechanisms and collapse angles of wall profile types with opening 10 (Giuffrè, 1993; D'Ayala and Speranza, 2003; Bazan and Meli, 2003; Milani et al., 2018).

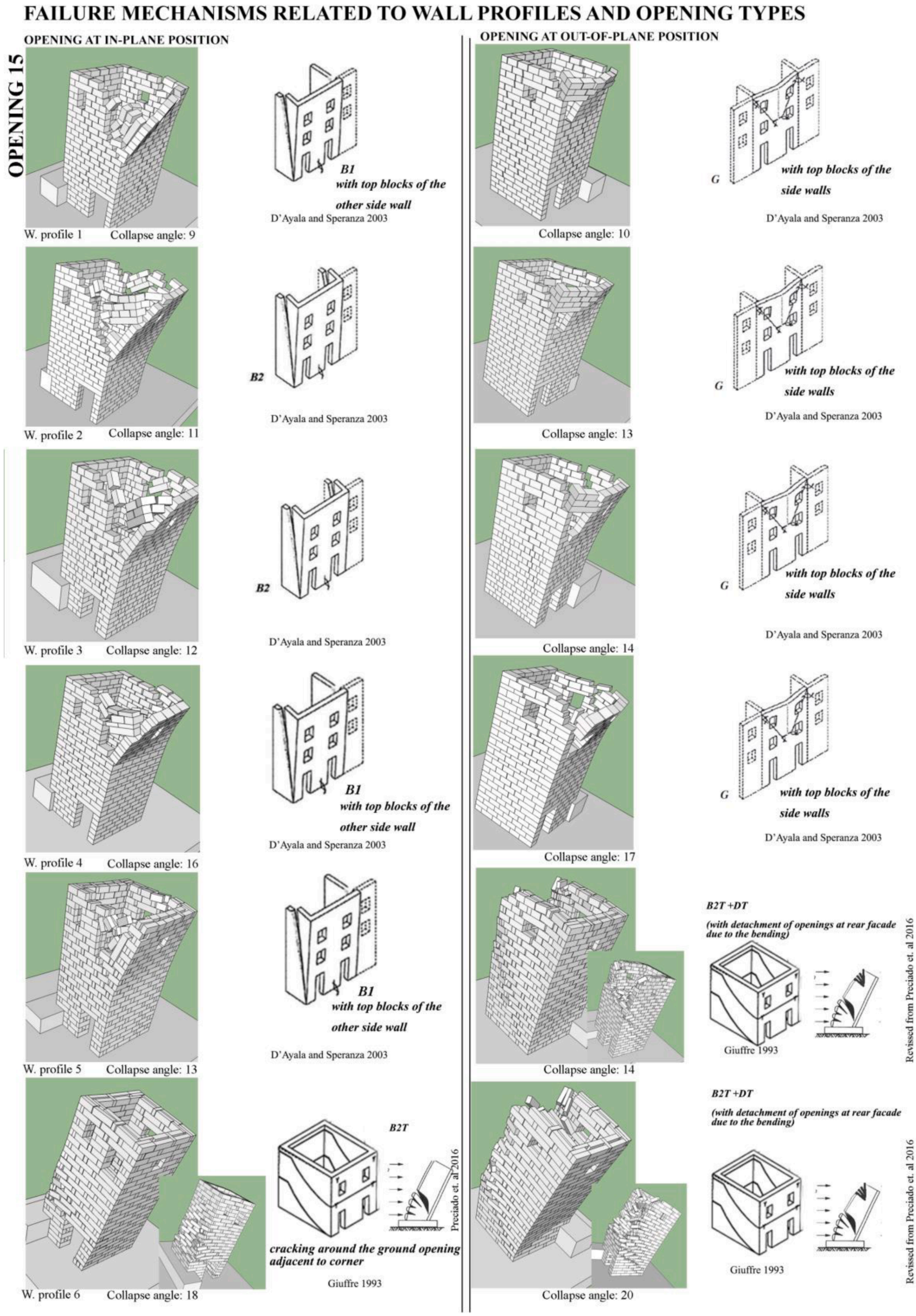

Fig. 7. Failure mechanisms and collapse angles of wall profile types with opening 15 (Giuffrè, 1993; D'Ayala and Speranza, 2003).

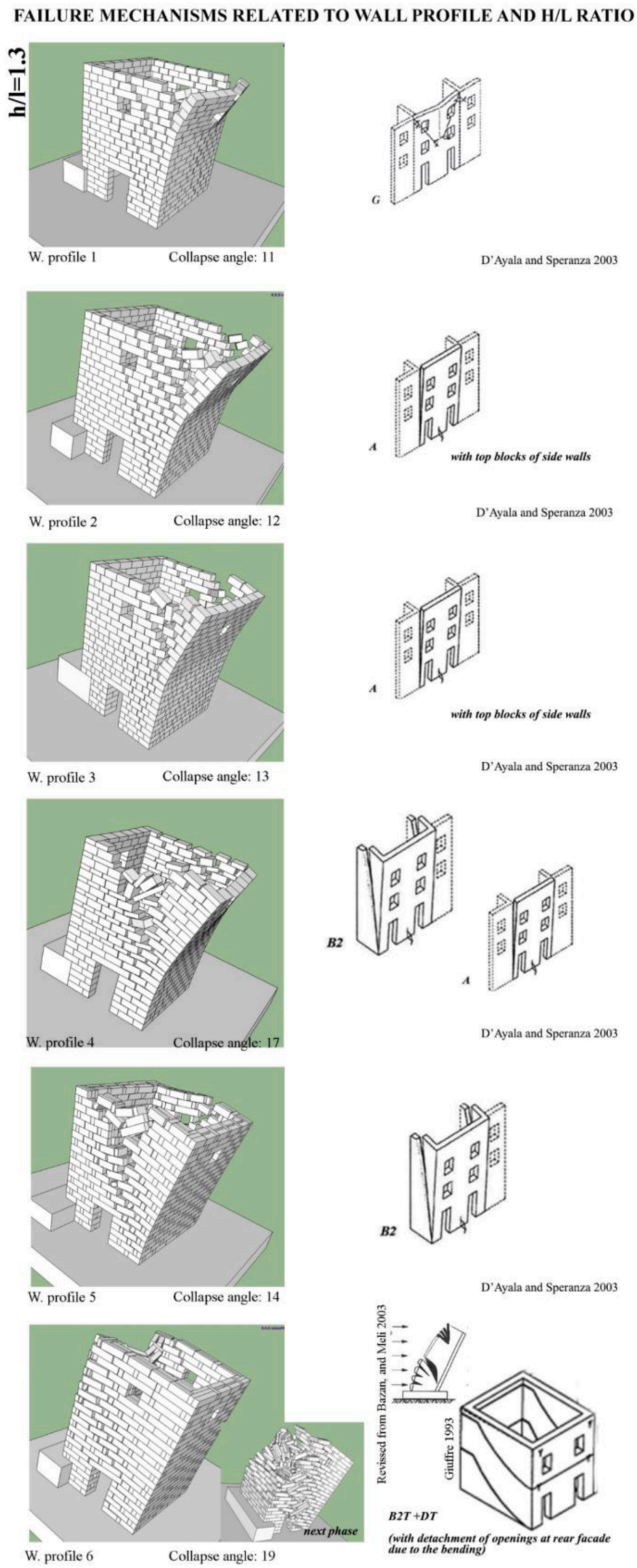

Fig. 8. Failure mechanisms and collapse angles of different wall profiles in different ratios (Giuffrè, 1993; D'Ayala and Speranza, 2003; Bazan and Meli, 2003).

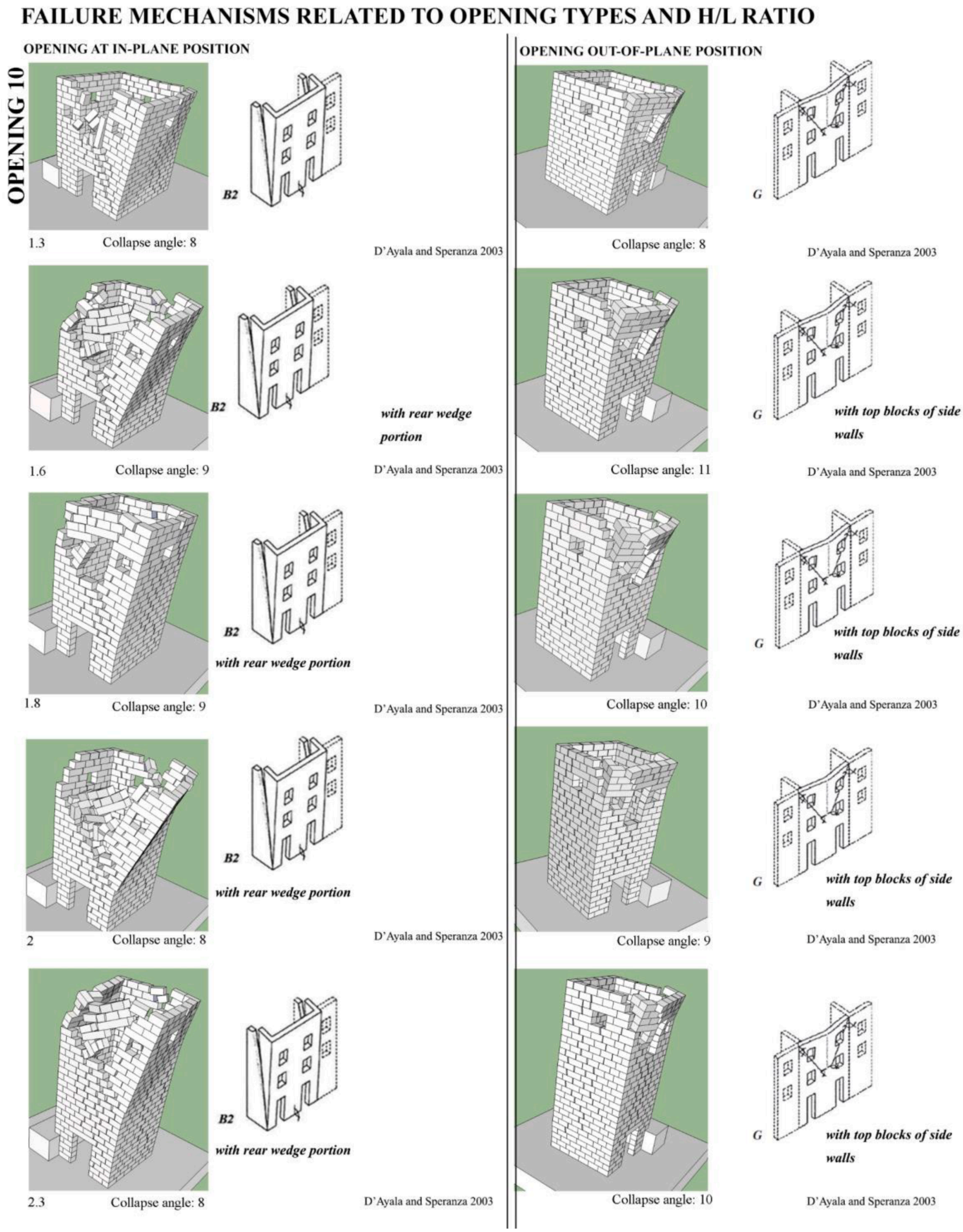

Fig. 9. The failure mechanism of wall profile 1 with opening 10 in different ratios (D'Ayala and Speranza, 2003).

5.1.1. Staggering ratio (s/h)

Staggering, which is the ratio between the horizontal distance between joints (s) and height (h) of the related course, is critical for the positioning of the stone blocks. The average staggering ratios for wall profiles varies between 0.4 and 1.8. According to the average resistance results, the staggering ratio is dominant in the determination of resistance. Wall profiles 1, 2, 3, and 4 are single leaf construction, while wall profiles 5 and 6 are double leaf construction, with header stones. However, regardless of the wall cross-sections, the resistance of the wall profiles increases proportionally to the staggering ratio, from 0.4 to 1.8. The wall profiles that have the highest staggering ratio are wall profiles 4 (s/h = 1.7) and 6 (s/h = 1.8) (Table 5). These profiles have the highest structural resistance, independent to any differentiation in their wall sections. While the usage of long blocks, up to 200 cm, increases the staggering ratio of wall profile 6, the usage of short blocks (height = 25–30 cm) in every two rows, increases the average staggering ratio of

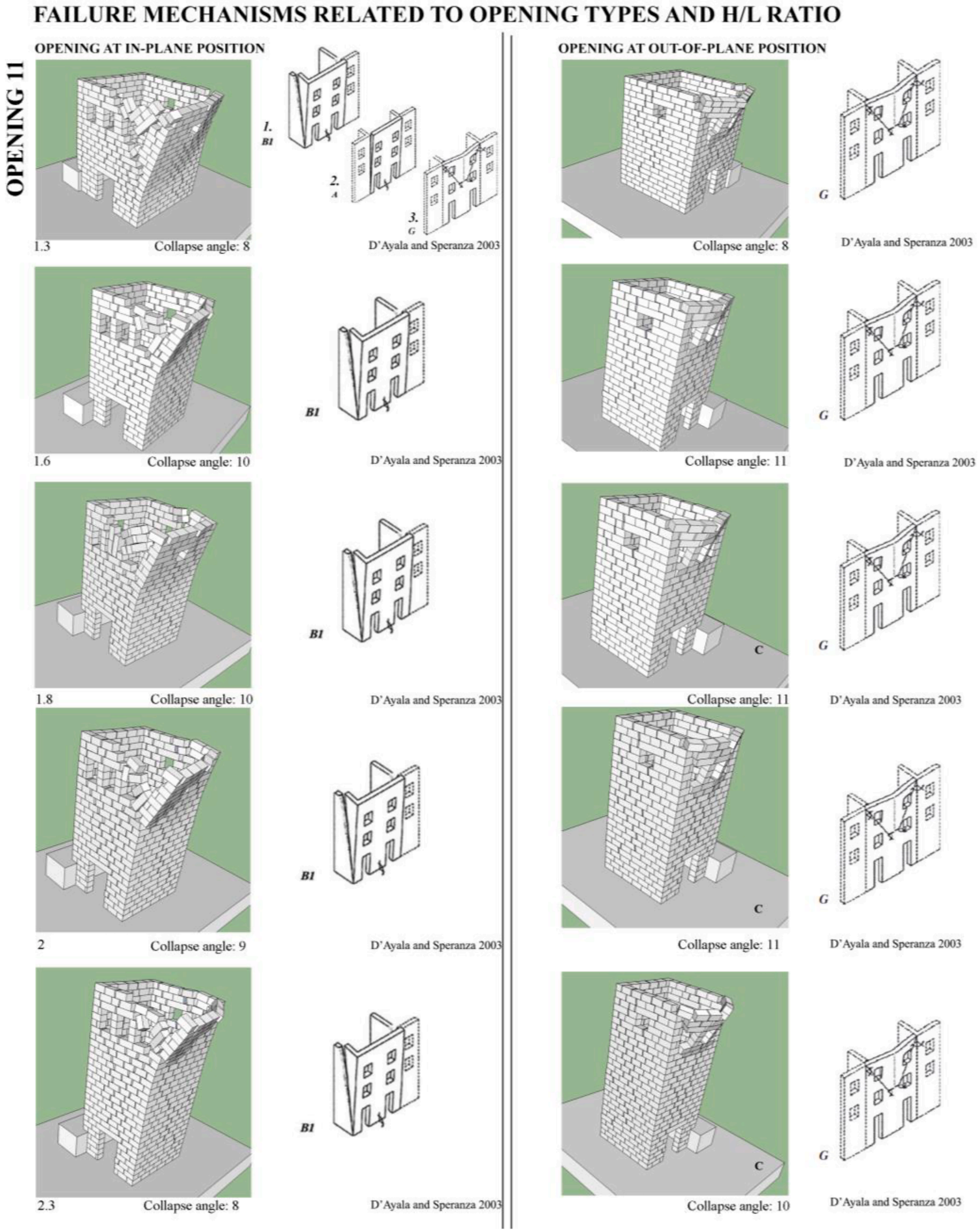

Fig. 10. Effect of opening 11 on failure mechanisms and collapse angles of wall profile 1 with different H/L ratios (D'Ayala and Speranza, 2003).

wall profile 4. In the analytical study of D'Ayala and Speranza (2003, 488), the staggering ratio from 0 to 1.8 increases resistance (λ) at h/l ratios between 1.25 and 2.5. This is similar to the results found in the case study towers.

The behaviour of wall profiles is not only related to staggering ratios. Wall profile 6 of double-leaf construction, demonstrates total body behaviour, while wall profile 4, of single leaf construction, demonstrates in-plane behaviour. In the studies of Jimenez (2011, 86), Restrepo-Velez et al. (2014, 10, 26) and Shi et al. (2008, 5–6), the single-leaf walls with staggering ratios of between 1 and 1.5 demonstrate in-plane failure mechanisms, similar to wall profile 4. The high staggering ratio strengthens the corner connections since it provides full interlocking of the corners to the sidewalls which results in in-plane behaviour. Thus, an appropriate double-leafed arrangement with headers results in total body behaviour, which in turn, increases structural resistance.

When the staggering ratio is less than 1, the out-of-plane failure

Table 5
Sub-qualities of characteristics types and their impact on failure mechanisms and collapse angles.

Impact of the wall profile	Organization of blocks		Wall section			Typical failure mechanism		Ave. resistance	
	Ave. s/h	Ave. Block l/h	Number of leaves	Upper stone depth	Usage of headers	Op. at in-plane	Op. at out-of-plane	Ave. collapse angle	λ
Wp. 1	0.4	1.5	1	60	–	B2 + A	G	9.3	0.16 g
Wp. 2	0.65	2	1	60	–	B2 + A	G	10.9	0.19 g
Wp. 3	0.8	2	1	60	Lower: 25%	B2 + A	B2 + G	12.7	0.22 g
Wp. 4	1.7	3	1	75	–	B2	B2	15.8	0.27 g
Wp. 5	0.8	2.4	2	50	Upper 11%	B2T + VS B2T + DT/	B2T + DT	13	0.22 g
Wp. 6	1.8	4	2	50	Upper 11%	B2T	B2T + DT	17.9	0.3 g

Impact of opening	Distribution	Distance to corner (cm)	Area (upper) (m^2)	Number (upper)	Common mechanism		Ave. decrease in c. angle / λ
					In-plane	Out-of-plane	
Op.1	Sym.	200–250	1	1	Typical mechanism of wall pr.	Typical mechanism of wall pr.	–
Op. 2, 5, 7, 9	Sym.	200–250	1.4–2	1 or 2	Typical mechanism of wall pr.	Typical mechanism of wall pr.	–
Op. 3, 4, 6	Asym.	50–60	1–2.5	1	Typical mechanism of wall pr.	Typical mechanism of wall pr.	–
Op. 8	Sym.	20–30	3	3	Typical mechanism of wall pr.	Typical mechanism of wall pr.	0.19 / 0.003g
Op. 12, 13	Asym.	50	1–1.5	2	Typical mechanism of wall pr.	Typical mechanism of wall pr.	0.21/ 0.003g
Op. 10	Sym.	20–30	7.4 (a large 5 m^2)	3	B2	G	1.02/ 0.02g
Op. 11	Sym.	20–30	3	3	B1	G	0.62/0.01g
Op. 14	Adj.	0	1	2	B2	G	0.69/0.01g
Op. 15	Adj.	0	2.95	2	B1	G	0.69/0.01g

mechanism (overturning of the facade due to vertical cracks at the corners) is observed in the single leaf wall profiles. The overturning of the out-of-plane facade wall occurs in wall profiles 1, 2, and 3, as their staggering ratios are between 0.4 and 0.8. A small staggering ratio weakens the corner connections. This is similar to the findings by Restrepo-Velez et al. (2014, 6) and Shi et al. (2008, 5–6), (small staggering ratio 0.7).

5.1.2. *The ratio between stone length and height (bl/h)*

When joints between blocks are located centrally between the upper and lower blocks, the ratio between stone length and height is directly proportional to the staggering ratio. This was illustrated by Shi et al. (2008, 5–6), where smaller blocks resulted in smaller staggering ratios. Decreasing both the staggering ratio and the length of the blocks results in a decrease in resistance and caused the out-of-plane failure mechanisms to occur, due to the poor corner connections. However, in this current study, joints between the stone blocks were not always positioned centrally and therefore, the average ratios of staggering and stone block dimensions were no longer proportional. As a result, bl/bh is examined separately. The results of the simulations demonstrated that larger block ratios increased the structural resistance of towers (De Felice and Giannini, 270, 2001; Giuffre et al., 267–271, 1994). Wall profiles 2 and 3 have the same block ratios, but different staggering ratios, resulting in different structural resistance. Analysis of block lengths alone or staggering ratio alone can be deceptive for dry masonry towers, in terms of structural resistance (Table 5).

5.1.3. *Usage of headers*

Headers are stone blocks laid perpendicular to the course wall and keep the wall leaves together. The systematic header stone distribution, namely providing a distance between each header stone so that they do not neighbour each other, and placing fewer header stones at the sides compared to the central area (3% at the edges and 8% at the middle); increases the monolithic behaviour of the two leaves and improves out-plane resistance. The tower fails via a total overturning, initiating with diagonal body cracking followed by horizontal cracking at the rear out-of-plane wall.

The wall profiles that have the highest resistance are wall profiles 6 and 4 due to their high staggering ratios. While wall profile 4, with a single leaf, demonstrates an in-plane failure mechanism, doubled leafed wall profile 6, connected with headers, demonstrates total body failure. When wall profile 5 (double leafed) and profile 3 (single leafed) with smaller staggering ratios (0.8) are compared with each other, wall profile 3 demonstrates out-of-plane failure, but wall profile 5 demonstrates full body behaviour with vertical splitting (Table 5). In literature, the effect of wall leaf connecting header stones on resistance against lateral force is generally studied using a wall portion without side walls (Ceradini, 1992; D'ayala, and Speranza, 480, 2003). In the study of Giuffre (1996, 117), Ceradini (1992), and De Felice (2011, 479), the number of header blocks in the wall section does influence the strength capacity. The interlocking between the external leaves of masonry is crucial to provide an out-of-plane seismic capacity. However, different wall profile types prove that the distribution and position of header stones and the relation of headers to each other is critical in terms of resistance and behaviour.

Wall profiles 5 and 6 are composed of header stones connecting the two outer leaves. They demonstrate total body behaviour. However, the resistance of wall profile 5 is lower than wall profile 6 due to its low staggering ratio. The low staggering ratio causes vertical splitting in addition to total body behaviour. If the header usage is supported with a high staggering ratio and high bl/bh ratio, the resistance increases, and the tower demonstrates total body behaviour (Fig. 5). Header stones used only in the lower part of the wall profile 3 cannot contribute to the resistance of the tower. Also, the header stone rows adjacent to each other alternating with stretcher rows reduce the strength of the towers considerably because they cause a decrease in staggering ratio. Wall profile 3 proves that headers can decrease structural resistance if they are used inappropriately (Table 5).

5.1.4. Stone depth

In single-leaf wall profiles, longer stone depths (75 cm) directly result in higher out-of-plane resistance, similar to the studies of Shi et al. (2008). Wall profile 4 has a longer stone depth (75 cm) when compared to wall profiles 1, 2, and 3 (60 cm). Wall profiles 1, 2, and 3 demonstrate an out-of-plane failure (G or DT). However wall profile 4 results in typical in-plane failure when openings are located in out-of-plane position (Fig. 5; Table 5).

5.2. Opening arrangement: area, position, and number

The subcategories of opening arrangements are the area, the number of openings, and the position of openings (Table 5). It was observed that the following actions all reduced the resistance of the structure to lateral loading: increasing the number of openings, increasing the area of the opening, and decreasing their distance to the corners of the structure.

Upper openings have an increased negative impact on structural resistance when compared to lower level openings. If a facade is composed of lower and upper openings, it is the upper opening that is taken into consideration. Although the lower openings are adjacent to the corner, they are not primary factors in determining the structural resistance and behaviour.

One or two symmetrical, or asymmetrical, openings up to 3 m^2 in the in-plane or out-of-plane position that do not reduce the resistance significantly are determined as 'negligible impact openings'. However, they can have an impact on behaviour depending on the properties of wall profiles (Table 5). These 'negligible impact openings' in the in-plane position generally result in the collapse of the side walls due to in-plane shear cracking in single-leaf wall profiles. In the study of Restrepo-Velez et al. (2014, 10), openings in the in-plane position with a staggering ratio of 0.8 cause diagonal cracks above the openings followed by the collapse of side walls, similar to that seen in wall profile 3. However, openings do not result in in-plane failure for wall profiles that have a staggering ratio smaller than 0.4, since the tower demonstrates out-of-plane behaviour due to the poor corner connection caused by small staggering. This failure mechanism occurs at low collapse angles and takes place prior to any potential impact caused by the openings.

'Negligible impact openings' (1–9 and 12&13) in out-of-plane positions generally result in the detachment of the out-of-plane facade wall. This was proven by the studies of Restrepo-Velez et al. (2014, 9, 20) and Vaculik et al. (2004, 4-5). In the cases considered in this study, however, the double-leaf and single-leaf wall profiles with large staggering ratios ($\geq$1.7) were not impacted by either one or two openings, so long as the openings were no larger than 3 m^2. Even though 'negligible impact openings' at the out-of-plane position changed the behaviour of the towers, they did not affect the resistance to lateral loading of towers.

'Significant impact openings' (10, 11, 14, and 15), in terms of resistance and behaviour, are those openings where the opening is greater than 5 m^2, or where there are more than two openings present or where the openings are located close to the corner of the tower (max. 30 cm). If openings are positioned close to the corner, or if there are more than two openings at the in-plane position, they result in in-plane cracking of only the side wall where the opening is positioned, followed by the collapse of the other side wall. Single-leaf wall profiles (wall profile 4) that have both high staggering ratios (1.7) and high stone depths (75 cm) are not affected by openings close to the corner: rather in-plane failure is observed, with the help of out-of-plane resistance (Table 5).

While a large upper opening, with an area more than 5 m^2, at an in-plane position causes the collapse of the side walls due to in-plane shear cracking, a large opening (>5m^2) at an out-of-plane position causes an out-of-plane failure regardless of the wall profile characteristics (Table 5).

5.3. Proportional relationship: ratio between height and length (H/L)

When the ratio between height and length is lower than 1.3 or higher than 2, both long (780 cm) or high facades (1405 cm) are being considered. High and long walls cause a decrease in resistance against lateral loading. While a higher h/l ratio does not affect the behaviour, at h/l ratios smaller than 1.3 the arch effect is introduced, resulting in the detachment of the out-of-plane wall with diagonal cracks, regardless of the wall profile type. In studies undertaken by Shi et al. (2008, 5), Restrepo-Velez et al. (2014, 7), Bui et al. (2017, 284-287), and Jimenez (2011, 77) it was shown that with decreasing h/l, the arching behaviour becomes more pronounced.

The effect the h/l ratio has on the resistance of dry masonry structures varies in relation to the staggering ratio. In the study of D'Ayala and Speranza (2003, 501), increasing the staggering ratio only produces an improvement in seismic performance for h/l ratios higher than 1. For example, the positive effect of high staggering ratio ($\geq$1.7) on behaviour is not observed at wall profiles 4 and 6 when the h/l ratios are smaller than 1.3. The towers demonstrate out-of-plane failure due to the arch effect and typical failure and no increase in resistance is observed.

5.4. Material usage: friction coefficient

Slight differences in the friction values of the stones (limestone: 0.72, granite: 0.6) did not affect the collapse angle or the behaviour of the towers. This result is supported by the study of D'Ayala and Speranza (2003). In this study, the effect of the friction coefficient between 0.6 and 0.8 on the collapse-load factor is constant (Fig. 11).

6. Conclusion

This study clarifies the sub-categories that have been found to have the most impact on the structural resistance of ancient dry masonry towers under lateral loading. These subcategories are staggering ratio, stone depth, the ratio between block length and height, proportional relationships between height and length, the area, number and position of openings, and the distribution of header stones. This study revealed that subcategories should always be considered in relationship with each other.

- Regular arrangement of stone blocks (staggering ratio (s/h) $\geq$ 1.7), where supported with appropriate block ratios (bl/h $\geq$ 3), increased the structural resistance of the towers.
- The advantage in the use of header stones has been observed, when appropriately positioned and used together with other blocks of appropriate dimensions (bl/h $\geq$ 3) and arrangements (s/h $\geq$ 1.7).
- Where rows with header stones were alternated with stretcher rows, the strength of the towers reduced considerably. This was due to a decrease in the staggering ratio in this arrangement (small staggering ratios s/h = 0.4).
- Upper openings had a much larger impact on structural resistance when compared to lower openings. Upper openings caused in-plane cracking at the upper parts of the facades, resulting in detachment of wall.
- Where there were less than 3 small-sized openings (100 × 100 cm, min 4.75 m cross-section) the collapse angles of the towers were not impacted either at the in-plane or the out-of-plane positions. However, they could alter the behaviour of the towers at the out-of-plane position.
- The towers with small staggering ratios (0.4) resulted in out-of-plane failure behaviour due to poor connections. These towers collapsed at small collapse angles (11 degrees), before any impact from the openings (up to 180 × 300 cm) occurred.
- In certain cases, the order that particular sub-categories impacted upon the behaviour of the structure changed. Large-sized openings (180 × 300cm) at minimum 4.75 and maximum 7.75 m plan cross-

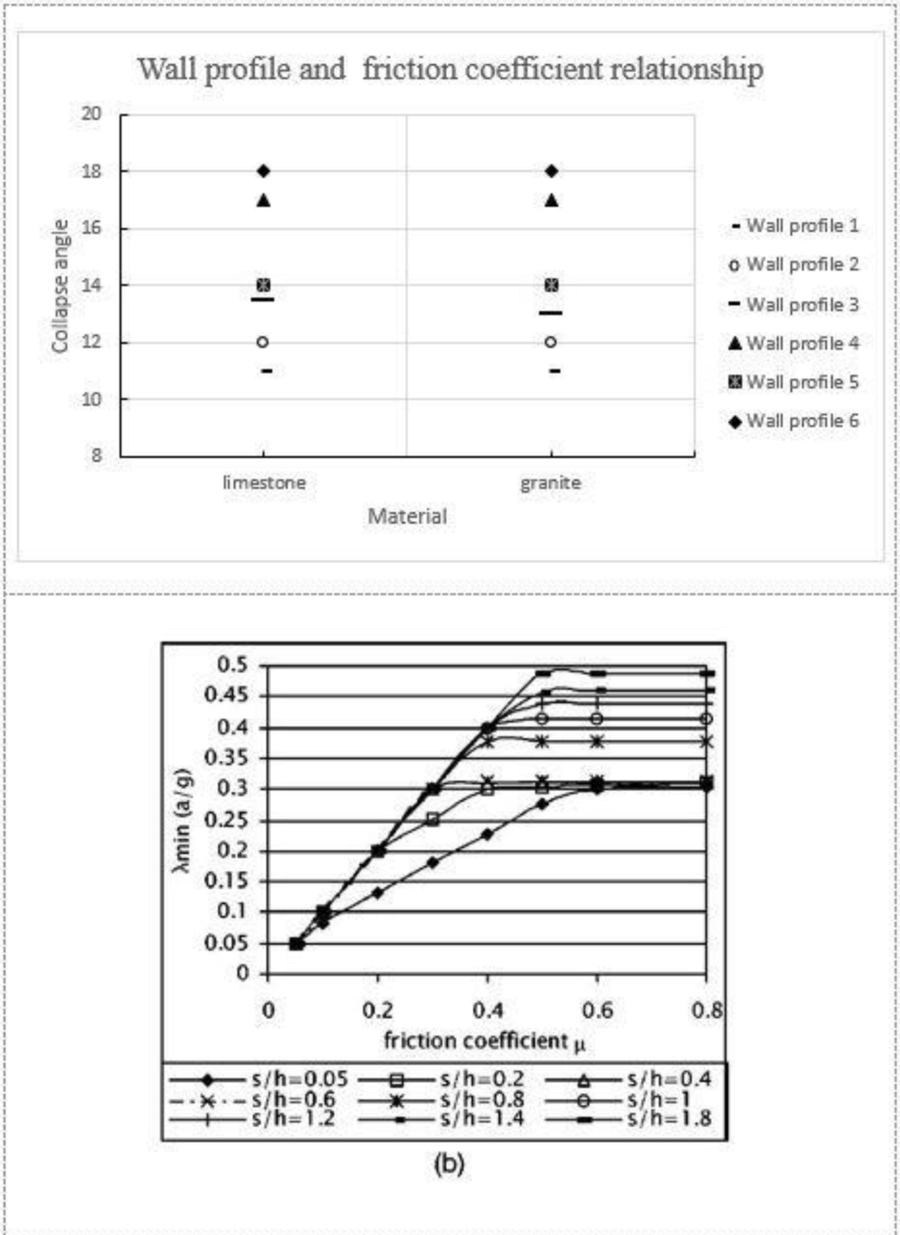

Fig. 11. Impact of friction coefficient on structural resistance (graph (b) from D'Ayala and Speranza, 2003).

section always became the dominant feature in all of height to length ratio towers modelled. However, small height to length ratios (1.3) became the dominant feature when compared to the impact resulting from small openings (50 × 75, 100 × 100 cm); or in towers with one or two small openings, or towers with one medium sized (140 × 210 cm) opening.

- Increasing staggering ratios ($s/h \geq 1.7$) resulted in an improvement of seismic performance, only for those structures where the h/l ratio was higher than 1.
- It appears that there was a standardization in ancient construction techniques for dry masonry towers. This was observed in the proportional relationships between wall height and length, as well as material usage. Although wall thicknesses altered, the height/length ratio remained between 1.6 and 2. These values provided minimum structural vulnerability for these towers.
- In terms of material usage, it has been observed that the blocks used in the construction of these towers; namely, granite and limestone; had similar coefficients of friction (0.6 and 0.72 respectively) and small changes in these values did not impact upon the structural behaviour and durability of the towers.

Understanding the structural behaviour of dry masonry towers makes it possible to propose restoration schemes through observing structural characteristics and failure mechanisms. This study provides a framework of vulnerability rankings with possible failure mechanisms that can be used to assess the stability of the masonry towers. This provides an understanding of the basic behaviour of the towers, enabling preventative measures to be developed.

It was seen that towers under high earthquake threat were designed with strong sub-categories as high staggering ratio, long stone depth or high block ratio, while there were no precautions against lateral loading in the towers under minimum earthquake risk. Precautions preferred in the construction of ancient towers prove that there might be awareness of earthquake risk status of their sites.

Declaration of Competing Interest

The authors declare that they have no known competing financial interests or personal relationships that could have appeared to influence the work reported in this paper.

Acknowledgement

This study has been supported by the Scientific Research Project Department of İzmir Institute of Technology, Turkey within the scope of the project, numbered 2016G_IYTE83.

References

AFAD. Türkiye Deprem Tehlike Haritası. Accessed March 5, 2018. https://www.afad.gov.tr/tr/26539/Yeni-Deprem-Tehlike-Haritasi-Yayimlandi.

Akarca, A., 1998. Şehir ve Savunması. Türk Tarih Kurumu, Ankara.

Azevedo, J., Sincraian, G., 2019. Modelling the Seismic Behavior of Monumental Masonry Structures. Last Modified 2000. Accessed March 5, 2019. http://citeseerx.ist.psu.edu/viewdoc/download?doi=10.1.1.111.6301&rep=rep1&type=pdf.

Bazan, E., Meli, R., 2003. Seismic design of buildings. Limusa Editorial, Mexico.

Bui, T., Limam, A., Sarhosis, V., HJiaj., M., 2017. Discrete Element Modelling of the In-Plane and Out-Of-Plane Behavior of Dry-Joint Masonry Wall Constructions. Eng. Struct. 136, 277–294. https://doi.org/10.1016/j.engstruct.2017.01.020.

Ceradini, V., 1992. Modellazione, Sperimentazione per lo Studio della Struttura Muraria Storica. PhD diss., University of Rome.

Colas, A.S., Garnier, D., Morel, J.C., Ciblac, T., O'Neill, C., 2016. Cross Curves of Stability for Dry Stone Retaining Wall Design. In Brick and Block Masonry-Trends, Innovations and Challenges, ed. D. P. Modena, and Valuzzi, 165-170. London: Taylor and Francis.

Concrete Institute, 1909. Transactions and Notes, 1–2. The University of Chicago, Chicago.

Da Costa, A.A.M.G., 2012. Seismic Assessment of the Out-Of-Plane Performance of Traditional Stone Masonry Walls. The University of Porto, PhD diss.

D'Ayala, D., Speranza, E., 2003. Definition of Collapse Mechanisms and Seismic Vulnerability of Historic Masonry Buildings. Earthquake Spectra 19 (3), 479–509.

De Felice, Gianmarco, Giannini, Renato, 2001. Out-of-plane seismic resistance of masonry walls. J. Earthquake Eng. 5 (2), 253–271.

De Felice, G., 2004. Out-of-plane Fragility of Historic Masonry Walls. In: Modena, C., Lourenço, P.B., Roca, P. (Eds.), Structural Analysis of Historical Constructions. Balkema Publishers, UK, pp. 1143–1148.

de Felice, Gianmarco, 2011. Out-of-Plane Seismic Capacity of Masonry Depending on Wall Section Morphology. Int. J. Arch. Heritage 5 (4-5), 466–482.

DeJong, M.J., 2009. Seismic Assessment Strategies for Masonry Structures. PhD diss., Massachusetts Institute of Technology.

Ferrante, Angela, Clementi, Francesco, Milani, Gabriele, 2020. Advanced numerical analyses by the Non-Smooth Contact Dynamics method of an ancient masonry bell tower. Math. Meth. Appl. Sci. 43 (13), 7706–7725. https://doi.org/10.1002/mma.6113.

Foti, D., Vacca, V., Facchini, I., 2018. DEM modeling and experimental analysis of the static behavior of a dry-joints masonry cross vaults. Constr. Build. Mater. 170, 111–120. https://doi.org/10.1016/j.conbuildmat.2018.02.202.

Giuffrè, A., 1993. Sicurezza e conservazione dei centri storici: il caso Ortigia: codice di pratica per gli interventi antisismici nel centro storico. Laterza, Roma.

Giuffre, A., Pagnoni, T., Tocci, 1994. In-plane Seismic Behavior of Historical Masonry Walls. Proceedings of 10th IB2 MaC: 263-272. Canada: Calgary.

Giuffrè, A., 1996. A Mechanical Model for Statics and Dynamics of Historical Masonry Buildings. In Protection of the Architectural Heritage Against Earthquakes, CISM Courses and Lectures (359), ed. V. Petrini and M. Save Udine, 71–152. Italy: Springer-Verlag.

Jay, B.A., 1908. The Mechanics of Engineering. Рипол Классик, Nizhegorodskaya Ulitsa.

Jimenez, D.D., 2011. Empirical Analysis of Masonry Walls: Structural Design and Seismic Reinforcement through Tilting Experiments. PhD diss., Massachusetts Institute of Technology.

McNicoll, A.W., 1997. Hellenistic Fortifications from the Aegean to the Euphrates. Clarendon Press, Gloucestershire.

Milani, G., Shehu, R., Valente, M., 2018. A kinematic limit analysis approach for seismic retrofitting of masonry towers through steel tie roads. Eng. Struct. 160, 122–228. https://doi.org/10.1016/j.engstruct.2018.01.033.

Preciado, A., Sperbeck, S., Ramírez-Gaytán, A., 2016. Seismic vulnerability enhancement of medieval and masonry bell towers externally restressed with unbounded smart tendons. Eng. Struct. 122, 50–61. https://doi.org/10.1016/j.engstruct.2016.05.007.

Restrepo Vélez, Luis Fernando, Magenes, Guido, Griffith, Michael C., 2014. Dry Stone Masonry Walls in Bending—Part I: Static Tests. Int. J. Arch. Heritage 8 (1), 1–28. https://doi.org/10.1080/15583058.2012.663059.

Romaro, F., 2011. A Study on Seismic Behavior of Masonry Towers. PhD diss., University of Trento, 2011.

Shi, Y., D'ayala, D.F., Jain, P., 2008. Analysis of Out-Of-Plane Damage Behavior of Unreinforced Masonry Walls, in: Proceedings of 14th International Brick & Block Masonry Conference. Australia: Sydney.

Shi, Y. 2016. Dynamic Behavior of Masonry Structures. PhD diss., University of Bath.

Synytsia, A., 2018. MSPhysics. Last modified November 16, 2017. Accessed May 5. https://sketchucation.com/forums/viewtopic.php?f=323&t=56852#p516427.

Vaculik, J., Griffith, M.J., Hogarth, J., Todd, J., 2004. Out-of-Plane Flexural Response Tests Using Dry-Stack Masonry, in: Proceedings of Australian Earthquake Engineering Society Conference, South Australia: Mt Gambier.

Vaculik, J., 2012. Unreinforced Masonry Walls Subjected to Out-Of-Plane Seismic Action. PhD diss., The University of Adelaide.